DEPARTMENT OF THE INTERIOR

U.S. GEOLOGICAL SURVEY

# Acid Rain Weathering of Salem Limestone: Surface Characterization of Control Material

by

U.S. Geological Survey
Victor G. Mossotti, James R. Lindsay[1] and
Michael F. Hochella, Jr.[2]

Open-File Report 86-366



[1]Menlo Park, CA [2]Dept. of Geology, Stanford University, Stanford, CA

## ABSTRACT

This report provides the baseline analytical characterization of the surface and bulk of freshly quarried Salem Limestone, and also the evaluation of several surface analytical techniques applied to rock weathering studies. The materials examined were selected from: (1) a control block which is being used in the National Acid Precipitation Assessment Program (NAPAP), and (2) from the stone yard at the National Cathedral in Washington D.C.

The surface analytical techniques evaluated included laser ionization mass spectroscopy (LIMS), secondary ion mass spectrometry (SIMS), Auger electron spectroscopy (AES), scanning Auger microscopy (SAM), X-ray photoelectron spectroscopy (XPS), and scanning electron microscopy (SEM) with energy dispersive X-ray analysis (EDX).

The insulating nature and thermal sensitivity of the Salem Limestone presented a particularly difficult problem for surface analysis with an electron or ion beam. Charge accumulation drastically reduced the yields of secondary ions, precluding the analysis of carbonate surfaces by means of SIMS. Laser ionization (LIMS) of the limestone, however, produced multicomponent mass spectra, but the data were not reproducible. In spite of surface losses of sulfur and carbon, useful Auger spectra were obtained and excellent SEM/EDX images and elemental analyses were recorded. Although the lateral resolution of XPS was relatively modest, the technique provided reliable chemical speciation information in the near-surface region of the Salem Limestone with no observed sample degradation.

The high calcium Salem Limestone contains fossil fragments with sparsely distributed grains of clays, silica, and heavy metal oxides. The use of XPS with sputtering for depth profiling revealed the presence of near-surface sulfur in the freshly quarried rock which appears to be disseminated over the calcite grain surfaces throughout extended regions of the sample. In the exposed limestone from the Washington National Cathedral stone yard, there is no evidence of near-surface sulfur, nitrogen or lead, elements often associated with anthropogenic activities.

# INTRODUCTION

The high calcium limestone quarried from the Salem Limestone formation in southern Indiana is a mineral resource that is virtually unlimited and of immense value. In the form of lime, it is an ideal soil neutralizer and is used as a flux in the processing of a number of commercially important ores for industrial metals. Large quantities of Salem Limestone are used daily by the paper and textile industries, and in a variety of ways by the chemical industry. It is also used in its native form by the glass industry. As a construction material, it is used for the building and maintenance of roads and in the manufacturing of portland cement. The most visible application for Salem Limestone has been as a building stone in a wide variety of structures and monuments; several notable structures include the Empire State Building, parts of the New York Metropolitan Museum of Art, the Rockefeller Center, the Pentagon, and the National Cathedral in Washington, D.C.

Because of its use throughout the United States as a building material, Salem Limestone has been selected as one of the materials to be included in the materials effects studies by the National Acid Precipitation Assessment Program (NAPAP 1983). Part of the NAPAP study is the assessment of mineralogical changes in building stone that have undergone exposure to various weathering processes for varying lengths of time. In this study, freshly quarried "control" stones believed to be relatively unaffected by anthropogenic processes (those associated with human activities) are being exposed at five different sites across the United States. By contrasting the changes in surface and bulk chemistry after varying periods of exposure, we hope to define those processes initiated by acid deposition, and to give estimates of stone damage directly related to human-caused acid deposition as separate from damage related to other weathering processes.

This report provides the baseline analytical characterization of the surface and bulk of freshly quarried clean Salem Limestone, and also the evaluation of several surface analytical techniques applied to rock weathering studies. As part of this effort, techniques such as laser ionization mass spectroscopy (LIMS), secondary ion mass spectrometry (SIMS), Auger electron spectroscopy (AES), scanning Auger microscopy (SAM), X-ray photoelectron spectroscopy (XPS or ESCA), scanning electron microscopy (SEM) with energy dispersive X-ray analysis (EDX), and powder X-ray diffraction (XRD) have been used for the characterization of the control materials. This analysis will include information on the distribution of mineral grains, compounds and elements. In addition, we also report the analysis of a weathered sample of Salem Limestone taken from the stone yard of the Washington National Cathedral[1/]. Although the weathered sample is not part of the NAPAP systematic study, the results of its characterization are useful for judging the type and extent of chemical alteration we can expect to observe in the materials undergoing planned weathering.

## HISTORICAL REVIEW

The greatest part of the literature on acid rain deals with its affects on soils and on components of the atmosphere, the limnosphere, and the biosphere (BUDIANSKY, 1981; BOYLE, 1983; BUBENICK, 1984); most of these publications focus on the environmental impact and health effects of acid rain (SHRINER et al., 1980). Reports on studies of acid rain weathering of building stones are scattered throughout the literature of a variety of disciplines including political, geochemical, the fine arts, architectural, and behavioral. Much of the pre-1978 literature on stone decay has been summarized in the anthology edited by Winkler (1978). The Winkler compendium includes contributions from seventeen recognized authors covering topics such as stone properties, stone weathering, and stone preservation; the treatment also includes comprehensive literature reviews in all of these areas. Another extensive literature review, specialized in the area of brick weathering, has been released by Hughes and Bargh (1982).

Numerous reports have appeared with examples of the deleterious effects of acid precipitation over wide areas of North America (LIKENS et al., 1974; COGBILL, 1976; GLASS et al., 1980, 1982; HILEMAN, 1981; SPICER, 1982; HOFFMAN et al., 1983), Europe (SEEGER, 1968; LONGINELLI et al., 1979; LIKENS et al., 1979), and other areas around the globe (SEQUEIRA, 1981). This phenomenon appears to be closely related to the accelerated deterioration of building materials and monuments worldwide (VIKTOROV, 1973; FURST, 1974; HOFFMAN et al., 1976; FASSINA et al, 1976; ROSSI-MANARESI, 1976; KALISER, 1976; GOUDIE,1977; GAURI, 1980; JEANETTE, 1980; SHARP, 1982; RABE, 1984).

It has been possible to measure weathering rates of building materials by photographic examination of inscriptions on tombstones (MEIERDING, 1981) and of aboriginal stone artifacts (WINCHELL, 1913). Such work indicates that weathering rates have accelerated over the last century and most dramatically over the past two decades, with the most pronounced weathering occurring in central urban areas. Such evidence indicts factors such as $NO_x$ from automobile emissions as a major contributor to acid deposition in urban areas, although the culpability of specific species is still difficult to quantitatively assess. A wide range of papers dealing with every aspect of atmospheric sulfur collectively present compelling evidence that $SO_2$ emissions have been related to changes in acid rain over the last twenty years (DAVIES, 1974; FREDIANA et al., 1976; EFES, et al., 1976; DRUFUCA, 1977; HUSAR, 1977; NRIAGU, 1978; HALES, 1979; FORREST, 1979; CARTER, 1979; BUDIANSKY, 1980; DE PENA, 1982). Some of this evidence is countered with arguments that other natural factors, such as organic acids and naturally-emitted sulfur and nitrogen compounds and alkaline dust, also affect the normal acidity of rain water (POUNDSTONE 1981, SEMONIN 1981). However, the contribution of natural factors to baseline pH seems to be at least qualitatively recognized in most assessments of acid rain.

1. The specimen was lying in the stone yard for several years after being quarried and cut in Bloomington, Indiana; thus, the stone was only affected by local weathering in Washington D.C.

The principles controlling the weathering of building materials are the same as those governing rock weathering in a geologic sense, and there exist a vast literature on this subject (CARROLL, 1970; LOUGHNAN, 1969; OLLIER, 1984 and references therein). Without question, the most damaging assault on building stone is from water, either pure water or water containing dissolved $CO_2$, $SO_3$, and oxides of nitrogen (WINKLER, 1966). Even water free of contamination directly hydrolyzes and dissolves the stone matrix. Water containing the sulfate ion, the most corrosive pollutant, attacks carbonate rock by direct dissolution action of sulfuric or sulfurous acid and/or by conversion of calcite to calcium sulfate. Water provides transport in and out of the stone for oxidizing and reducing agents, acids, bases, chelating agents, and microorganisms. Microorganisms contribute to the dissolution process by naturally acidifying the moisture on the stone and by generating ligands that form complex ions with the dissolved minerals. The deterioration of stone may be accelerated by a high content of expandable clay minerals (DAVISON, 1978; DEMEDIUK, 1960; FISHBURN, 1940; FREEMAN, 1966; FREEMAN et al. (1967). Temperature excursions, especially temperature cycles across the freezing point of water, exacerbate the damaging effect of water by enlarging pores and cracks in the stone. As the matrix of the stone dissolves, more resistant mineral grains are loosened, and the strength and gross dimensional features of the stone are altered.

In summary, stone weathering is initiated by external physical and/or chemical attack on the individual grains of the stone. But it is conceivable that once the weathering of certain mineral grains has been initiated, the reaction products can attack neighboring grains which otherwise would have been relatively inert to the external weathering agent. For example, such weathering mechanisms might be expected in the neighborhood of pyrite and marcasite grains which have been shown to generate sulfuric acid on oxidation (KELLER, 1966; WINKLER, 1973 p.142). To understand stone weathering at the microscopic level, we consider it essential that techniques be used that will permit the measurement of chemical alteration of individual mineral grain surfaces and their short range environment.

## EXPERIMENTAL PROCEDURE

### Sample Preparation

Four samples were examined in the study. Three samples were taken from the freshly quarried Salem Limestone study block; the fourth sample was obtained from the stone yard of the Washington National Cathedral. The quarried specimens used in this work were cut from 2 (or 4) x 12 x 24 inch slabs from a block measuring 42 x 48 x 100 inches; a detailed description of the Salem Limestone study block and its preparation and cutting procedure is given in ROSS and KNAB (1984). Each slab was assigned a two-letter, one-digit number designation to identify its position in the study block. The samples used in this study are AU-3, HU-3, and NU-3 taken from the top, middle, and bottom of the study block, respectively. The slabs in turn were cut into smaller briquettes measuring roughly 2 x 3 x 3 inches. The hand specimens were then sliced with a water lubricated diamond saw into pieces about 1mm thick such that the cut faces were oriented parallel to the

bedding planes of the limestone formation. The results of the limestone characterization reported below indicate that the bulk and surface chemistry, and the general petrography of the three control samples were closely matched. Accordingly, we feel confident that the control samples selected for study are representative of the control block.

Several samples that may have been contaminated during handling were cleaned by submersion in a dilute high-alkaline phosphate detergent solution in an ultrasonic cleaner for about 10 minutes. Following this, the samples were thoroughly rinsed in distilled water. The samples were then boiled in acetone and ethanol for five minutes each and finally were oven dried at 110°C for 30 minutes. It became apparent that the detergent cleaning was affecting the surface chemistry of these samples. Therefore, the detergent solution cleaning step was dropped, and the samples were cleaned only in acetone and ethanol. These solvents are used to degrease the samples, and analysis of a few specimens rinsed only in distilled water showed that they did not alter the surface chemistry of the minerals in these stones except to remove possible gross contamination. The sample from the stone yard of the Washington National Cathedral, labeled NC-1, was cut and cleaned in the same fashion as the quarried rock; both freshly cut and exposed surfaces were analyzed.

Bulk analysis

Major and trace element analyses for the Salem Limestone study block were performed using conventional atomic absorption (AA), inductively coupled plasma (ICP), and dc-arc optical emission techniques (OES). X-ray powder diffraction patterns were run on a computer controlled Rigaku X-ray diffractometer. EDX analyses were performed with a Tracor Northern 5500 X-ray energy dispersive system in conjunction with the SEM work described below; the excitation volume of EDX, a function of the sample morphology, sample material, beam energy and beam diameter, was a hemisphere with approximately 2 um diameter.

Surface analysis

Because stone weathering may be initiated by chemical attack on individual mineral grain surfaces, we chose to evaluate techniques that collectively could provide chemical speciation information from highly localized surface-most atomic layers of a sample.

Scanning electron microscopy (SEM)/energy dispersive X-ray analysis (EDX): Conventional secondary and backscattered electron imaging was performed on a Cambridge Model 250 Mark-II SEM with the samples carbon coated. Except for the possible volatilization of sulfur, no apparent sample damage was evident with beam conditions typically set at 20 kV and 300 uA. This is in keeping with earlier reports on the specific application of SEM to the examination of limestone and marble surfaces (ASMUS, 1978; LEWIN and CHAROLA, 1978). The imaging resolution of SEM under the conditions used in this work was less than 0.01 um.

X-ray photoelectron spectroscopy (XPS): In XPS, often referred to as electron spectroscopy for chemical analysis (ESCA), core-level X-ray photoelectron spectra can provide compositional and oxidation state information on the near-surface atomic layers of a material to a depth as great as 5 nm. For a general review of XPS including theory and instrumentation, the reader is referred to HERCULES and HERCULES, 1974, and to RIGGS (1975). General applications of XPS have been reviewed by HERCULES, 1976, and applications in the area of geochemistry have been reviewed by BANCROFT, et al. (1979). Specific examples of the use of XPS in rock weathering studies can be found in the publications by PETROVIC, et al. (1976), BERNER and HOLDREN (1979), HOLDREN and BERNER (1979), SCHOTT et al. (1981), BERNER and SCHOTT (1982), and SCHOTT and BERNER (1983).

Two sets of XPS experiments were conducted, the first with a VG ESCALAB Mk II, and the second set with a Perkin-Elmer Series 5400 ESCA; the latter instrument afforded a lateral resolution of approximately 200 um, a factor of ten better than the VG instrument. The vacuum during data collection for both instruments was in the low $10^{-11}$ to high $10^{-12}$ Pa range. XPS spectra for both instruments were obtained using a non-monochromatic Al X-ray source (Al K = 1486.6 eV) operated at 300-600 watts in conjunction with a hemisperical analyzer; a silver standard and a sample of Iceland Spar were used for calibration.

The photoelectron peaks in the raw XPS spectra of Salem Limestone were normal in shape and width but shifted to higher binding energies by approximately 6 eV. Because the positive surface charging was static, instead of utilizing the charge neutralizing electron flood gun, we corrected the spectra mathematically using the average difference between the observed line positions and the reported energies for the O1s (530.9 eV) and $Ca2p_{3/2}$ (346.8 eV) lines for calcite (Wagner et al., 1979). Survey spectra were collected in constant analyzer energy (CAE) mode with a pass energy of 50 eV over the range of binding energies from 0.0 to 1000.0 eV (step size 1.0 eV). Narrow band spectra were collected similarly, but with a step size of 0.1 to 0.2 eV and with a pass energy of 20 eV. The Perkin-Elmer instrument was operated under similar conditions as the VG instrument except for the smaller area of analysis.

The XPS observations were augmented by intermittent argon-ion sputtering as a means of obtaining additional information on the depth distribution of sample constituents. This is discussed in more detail in the discussion section.

Auger electron spectroscopy (AES)/Scanning Auger microscopy (SAM): Auger electrons can be excited by either X-rays or, more efficiently, by an electron beam; the fundamental principles and applications of Auger spectrometry have been reviewed by JOSHI, et al., 1975 and by RIVIERE, 1983. Electron-beam excitation of Auger electrons is favored since an electron beam can be electromagnetically or electrostatically focused for high lateral resolution on the sample surface. This property of electron beam excitation is fully exploited in the SAM technique, in contrast to conventional AES which uses a diffuse beam of electrons for sample excitation.

Thus far, AES/SAM has found relatively limited application to the analysis of geological materials, although several examples have been reported (see, eg., MUCCI et al., 1985; MACKINNON and MOGK, 1985; and BISDOM et al., 1985). For a discussion of the attributes and limitations of high spatial resolution AES/SAM applied to the analysis of mineral surfaces, the reader is referred to HOCHELLA, et al., 1986a,b.

As with XPS, two sets of AES/SAM experiments were conducted, the first with the VG ESCALAB Mk II system, and the second set with a Perkin-Elmer Phi-600. The VG instrument afforded a lateral resolution of approximately 0.2 um at 1 nA beam current; the Phi-600 provided a 35 nm beam at 0.05 nA. To obtain usable Auger spectra on Salem Limestone, we raster-scanned the electron beam over areas 0.1 x 0.1 mm or larger at 3 to 5 kV and up to 20 nA of sample current. Beam currents were not directly measured. The sample was also tilted in the beam in order to increase secondary and backscattered electron emission to help balance the influx of non-backscattered primary electrons (HOCHELLA et al., 1986a). We were able to obtain Auger spectra with a reasonable signal-to-noise ratio and no peak shifts at a tilt angle (the angle between the sample normal and the electron beam) of between $45^{o}$ and $55^{o}$. At a constant beam setting, an increase in sample angle dramatically decreased sample charging. Survey spectra were collected from 0.0 to 1000.0 eV kinetic energy in constant retard ratio (CRR) mode.

Secondary ion mass spectrometry (SIMS): The SIMS technique relies on a focused beam of ions for surface sputtering and secondary ionization. The ions released from the surface are collected by a mass spectrometer, providing analytical information on all elements of the periodic table. Although the technique is destructive to the surface, the primary ion beam can be controlled such that successive atomic layers can be systematically removed from the surface, providing a depth resolution of 15 nm ($O_2^+$) to 25 nm ($Cs^+$); lateral resolution of the sampled area on the surface is typically 40-50 um, but can be as small as a few microns. For recent references concerning the use of SIMS in geologic applications, see MCKEEGAN et al. (1985) and references therein.

Experiments were conducted with a Cameca IMS-3F SIMS spectrometer. Positive and negative ion spectra were collected with $O_2^+$ and $Cs^+$ primary ion excitation, respectively. Samples were studied with and without a gold coating. Beam conditions were adjusted to maximize the fraction of neutral species to minimize sample charging.

Laser ionization mass spectrometry (LIMS): The LIMS technique uses a focussed laser beam for sample ablation and ionization; a time-of-flight mass spectrometer provides analysis for isotopes and molecular species. Since the depth resolution of the technique is measured in micrometers, LIMS should be considered a microanalytical technique rather than a surface analysis method. An example of the application of LIMS for in situ isotopic analysis of mineral grains has been reported by SUTTER AND HARTUNG, 1984. For a general overview of LIMS, the reader is referred to a paper by HEINEN AND HOLM, 1984. Our experiments were conducted with a Cambridge Mass Spectrometry Ltd. LIMA-2A instrument.

## RESULTS AND DISCUSSION

### Evaluation of analytical techniques

It is well known that chemical and structural artifacts can be induced in a target area when energy is transferred to the atomic framework of a surface by particle bombardment. The extent and type of induced damage depends on the nature of the irradiation used for surface excitation, on the flux-density of the irradiation, on the time of surface exposure, and on the chemical composition and structure of the material being examined.

Excitation with electrons (SEM/EDX and AES/SAM): Electrically nonconducting materials, and especially those with low heat conductivity such as the Salem Limestone, present a particular challenge for analysis with a beam of charged particles. The build-up of sample charge during irradiation results in line broadening in the electron energy spectra, and elevated local temperatures on the surface can result in structural and stoichiometric alterations of the surface within the excitation volume.

Fig. 1a shows the differentiated AES spectrum of study block sample HU-3 observed under low lateral resolution conditions (2 x 2 mm) with the VG instrument. Although peaks due to the major elemental constituents (C, Ca, and O) are clearly evident, the signal-to-noise ratio in the spectrum is insufficient to show minor element peaks. Fig. 1b shows a high spatial resolution SAM spectrum of HU-3 taken with the Perkin-Elmer instrument. It is notable in Fig. 1b that the carbon peak is altogether missing, an example of electron stimulated or possibly thermally stimulated carbonate decomposition (BRAUN, et al. 1977). Such stoichiometric alteration under high current density conditions precludes the main advantage of SAM over XPS. For example, the threshold for calcite decomposition for a 3 kV, 10 nA beam occurred when the beam was rastered over a tagret area less than approximately $10^4$ $um^2$.

Because the SEM/EDX technique is not very sensitive to elements with atomic number less than 11, and because the excitation volume of the method precludes its use as a surface sensitive technique, coating the sample surface with a layer of carbon to render the surface conducting does not lead to any loss of information. We found SEM/EDX could provide high lateral resolution imaging of individual limestone grains and semiquantitative bulk elemental analysis of grains larger than 2-3 um. Similarly, we found backscattered electron imaging of great value in locating non-carbonate grains.

Excitation with ions (SIMS): $Cs^+$ ion bombardment was used for the production of negative ion mass spectra and $O_2^+$ ions for the production of positive ion spectra. Without the use of gold coating on the sample, the ion yields in our experiments were insufficient for the detection of any analytical signal in both positive and negative ion spectroscopy. Even with the samples gold coated, secondary ion yields were just barely sufficient for the detection of oxygen in the negative ion spectrum and calcium in the positive ion spectrum.

Excitation with photons (LIMS and XPS): When electromagnetic energy is dissipated into the sample surface, electronic defects can be induced which can destabilize existing compounds and can result in new compound formation. Examples of photon induced damage include the reduction of high valency transition elements, eg., $Cr^{+6}$ to $Cr^{+3}$ in dichromate, and the desorption of oxygen and $CO_2$ from oxides and carbonates, respectively (see COPPERTHWAITE, 1980 for a review of photon induced surface damage). Fortunately, the great majority of salts, oxides, and metals show no damage, even with long irradiation time.

Our experience with X-ray photoelectron spectroscopy indicates that calcium carbonate surfaces are stable under X-ray excitation. XPS provides readily interpretable information on chemical species in the surface-most atomic layers of a material, although the lateral resolution is typically limited to approximately 200 um. Although detailed knowledge of the lateral distribution of an element is strictly limited by the resolution of the technique, under certain circumstances a general picture of the elemental distribution can be inferred from controlled surface sputtering followed by XPS measurements. This tactic is discussed in some detail below in our accounting for sulfur in Salem Limestone.

A serious limitation of XPS, AES/SAM, and SEM/EDX, at least when such methods are applied to limestone samples, is that the methods all require relatively high atomic concentration of the analyte in the excitation volume for detection. We estimate that analytical sensitivities for the limestone samples are in the range of one atomic percent for these techniques. For this reason, and because SIMS analysis was not successful, LIMS was considered as a technique that potentially could provide trace level concentration data from a localized region of the sample. Unfortunately, the poor optical imaging of the sample made it difficult to identify the area targeted for the laser pulse. Moreover, the nonreproducibility of the LIMS results and the poor mass/charge resolution limit the analytical value of the method for our purposes.

In summary, LIMS and SIMS are precluded as techniques for the analysis of carbonate surfaces, even with the most sophisticated sample handling techniques. SEM/EDX provides high lateral resolution imaging and bulk elemental analysis of localized areas; consequently, SEM/EDX is valuable for overall sample reconnaissance. The XPS technique provides valuable chemical speciation information from the surface-most atomic layers of limestone materials with no induced surface damage. Moreover, the combination of XPS and ion sputtering can be used to obtain data on the depth distribution of chemical species. If lateral resolution is sacrificed, AES/SAM also can be used for the analysis of limestone surfaces.

Limestone characterization

The Salem Limestone control samples consist of the fossilized debris of marine organisms; most of the fragments observed in thin section are 0.2 to 1.0 mm long. The depositional environment and the sedimentology of the Salem Limestone formation have been thoroughly described by SMITH (1962) and DONAHUE (1967). Major and trace element analyses of the Salem Limestone control samples are given in Tables 1 and 2, respectively.

The X-ray diffraction patterns of samples NC-1 (National Cathedral) and HU-3 (middle of the quarry block) were identical. A computer search/match routine matched all lines with the calcite pattern, except one line just above background which was identified as the major quartz peak (26.65° 2θ). There was no indication of dolomite or of any other phase in the samples from the diffraction patterns. However, a number of other phases were found by SEM/EDX.

The SEM photographs in Figs. 2-3 illustrate a morphological feature, typical of all samples examined, in which calcite grains are concentrically disposed to approximate an oölitic texture; both the core and rind of the oöids in all samples consist principally of calcite grains up to 3 um diameter. The oöid rinds are relatively thin compared with the diameters of the cores, and the oöid shapes are usually more oblong than oval. SMITH (1966), suggests that the Salem Limestone is not true oölitic rock since it it not composed of well formed oöids. In contrast to Fig. 2a, the weathered Washington National Cathedral sample of Fig. 3 shows the oöid rinds to be more eroded and the pores more filled than in the control samples.

Because of the basic mono-mineralic nature of this limestone, backscattered electron imaging was important in locating non-carbonate grains, even though the roughness of the surface resulted in noisy images. The distribution of various clays and oxide grains is sparse throughout the oöid cores; impurity grains appear to be altogether absent in the oöid rinds. Figs. 4a and 4b show secondary electron and backscattered electron images, respectively, of sample NU-3 with a high-iron mineral grain in the center of the figure and a silica fossil fragment near the top of the figure. Because the backscatter coefficient for silica is less than that for calcite, the silica fossil is not visible in Fig. 4b; EDX showed only iron in the inclusion and silicon in the fossil fragment. Additional heavy metal grains analyzed by EDX contain Sn, Cr, and Pb. We believe the heavier metals (Fe, Sn, Cr and Pb) are present in the form of oxides or carbonates since these elements appear to have no association with sulfur in the samples examined. This is discussed in greater detail in the following paragraphs on XPS results.

An XPS spectrum typical of the Salem Limestone study block samples is shown in Fig. 5 for HU-3; the 60-190 eV and 275-295 eV binding energy regions are shown in the high resolution scans in Figs. 6 and Fig. 7, respectively. All XPS spectra of the study block samples show Ca, O, C, and Mg lines with relative intensities indicative of $CaCO_3$ with a minor Mg (dolomitic) component. Varying amounts of minor N, Na, Al, Si, P, S, Fe and Pb were also detected on the surface of these samples (cut-surfaces and "as received" surfaces). The Al and Si lines, attributed to minor amounts of clay and silica, is substantiated by SEM and EDX data. The lines due to the heavier metals (Fe and Pb) also confirm the EDX observations.

In accounting for the sulfur, we have no SEM or XPS evidence for the presence of sulfides. The energy of the S2p line in Fig. 6 (168.2 eV) is actually close to that of a metal sulfate, 5 to 7 eV higher than that expected for a metal sulfide (WAGNER et al., 1979). This observation is consistent with the work of PERRY et al. (1983, 1984) and HOCHELLA et al. (1986b) which shows that metal oxides and sulfates appear on sulfide surfaces due to atmospheric exposure. Accordingly, although we can not completely rule out the the presence of sulfide grains, we feel that if any such grains exist in the sample, they are present in extremely low abundances.

There are at least three possibilities for the distribution of sulfur. The sulfur can be highly localized in sulfate or sulfide grains. The sulfur can be widely distributed over many grains. And finally, a combination of the first two special distributions could exist. If the sulfur is globally distributed over the surface of the calcite grains, the XPS sulfur signal will decrease as the near-surface atomic layers are removed by sputtering. If the sulfur is highly localized in grains, the signal should remain unchanged or increase, possibly with a chemical shift depending on the oxidation state of the sulfur within the grain. And finally, if the combination distribution exists, the signal will probably decrease to a constant level on sputtering.

A simple sputtering experiment was conducted to augment the analytical data on sulfur. A sample of HU-3 was argon-ion sputtered at 4 kV accelerating potential with the Perkin-Elmer 5400 ESCA. The approximate surface removal rate at this energy for $SiO_2$ on Si is 6-7 nm/min. Although the removal rate for carbonates has not been calibrated for this instrument, it is likely to be within a factor of 3 of that for $SiO_2$. After the first 30 seconds of sputtering, the S2p line intensity was undetected above the background (Fig. 8a and Fig. 8b). This experiment suggests that the sulfur is widely distributed over the calcite grains but confined to the near-surface atomic layers.

The Na and P were only observed on the study block samples that were in contact with a mild detergent solution used to degrease the samples for ultra-high vacuum compatibility, and we believe that their presence is due to adsorbed alkali phosphates from the detergent. The energies of the Nals photopeak and the Na KLL Auger electron line give an Auger parameter of 573.5 eV which is within 1 eV of that observed for $NaPO_3$ (WAGNER et al., 1979). Samples cleaned with a highly diluted detergent solution showed only Na and no P. Samples cleaned in only acetone and ethanol had no surface Na or P.

The XPS chemical shift, evident in Fig. 7 for the carbon 1s spectrum, allows us to differentiate between the carbon due to air exposure and the carbon in the $CO_3^{2-}$ groups of the calcite structure. The signals from the carbon in the calcite and the carbon contaminant are at approximately 289 eV and 284 eV, respectively (SOMMERS, 1975). The contaminant carbon species most likely present, based on the mass spectrometry of evolved gasses from oxide surfaces when heated, are CO and $CO_2$ (STEVENSON and BINKOWSKI, 1977). The peak due to the contaminant can be eliminated by a small amount of sputtering, or depending on surface roughness, can be enhanced by tilting the specimen in relation to the electron energy analyzer to increase the surface sensitivity of the technique, i.e., angle resolved XPS.

Small amounts of nitrogen were found on the surfaces of many of the samples studied. All evidence suggests that this nitrogen is from air contamination affecting only the top one or two monolayers of the surface and not a result of nitrates that may be dissolved in ground or rain water that have come in contact with the surfaces of these grains. This conclusion is based on a sputtering experiment similar to that conducted for sulfur. Although uniform sputtering is impossible on a rough surface, a sample of HU-3 was argon ion sputtered in the VG instrument twice for 1 minute periods at 1 kV accelerating potential. The approximate removal rate

for the ion gun on the VG instrument at this energy is 0.7 nm/min. The carbon contamination was removed at the same rate as the nitrogen, and after the first minute of sputtering, the N 1s line intensity was less than one standard deviation above the background. This amount of nitrogen can be attributed to 'knock-in' effects of the bombarding argon ions. After the second minute of sputtering, no nitrogen was detected. This sputtering experiment suggests that the nitrogen is mixed with the carbon contaminants and is confined to the top few tenths of a nanometer of the surface. Additionally, when samples still wet with ethanol were inserted into the instrument, effectively eliminating air exposure after cleaning, the presence of nitrogen was reduced or eliminated on these surfaces.

The National Cathedral (NC-1) samples showed the same presence or absence of Na and P depending on contact with the detergent solution. However, in contrast to the study block samples, no heavy metals were seen in the spectra of the cut or exposed surfaces, and no sulfur was detected. Si and Al were only detected in one of the four NC-1 samples studied. It is tempting to speculate that non-carbonate grains and impurity elements may have been flushed from NC-1 during its exposure in the Washington National Cathedral stone yard. If such an assessment is valid, these observations should be confirmed by the analysis of NAPAP samples that have undergone weathering for varying lengths of time. Such a study is currently underway.

## CONCLUSIONS

In this study, we have evaluated a variety of analytical techniques for the study of carbonate surfaces, and in the process, have characterized the bulk and surface chemistry of the Salem Limestone control block used in the National Acid Precipitation Assessment Program.

This study is based on the notion that under given conditions, individual grains in the stone will weather differently depending on their respective chemical composition and on the weathering products of neighboring grains. Hence, the key to understanding stone weathering must be based on observations of surface alterations of individual grains. Accordingly, high lateral resolution instrumental techniques sensitive to elemental oxidation states and which can differentiate signal originating at near-surface atomic layers from the bulk signal will be required for this work. Because of surface damage induced by the probe beam, no single technique appears to meet these needs for carbonate surfaces. Attempts to use scanning Auger electron spectroscopy for high lateral resolution work (submicrometer) resulted in decomposition of the carbonate matrix. Low positive and negative ion yields precluded the application of SIMS in this work, and the non-reproducibility and poor lateral and depth resolution of LIMS rendered such data virtually useless. However, the combination of XPS and SEM/EDX with intermittent surface sputtering have proven invaluable in this application.

The control samples are made up almost entirely of fossil fragments consisting of calcite grains partially organized into oöid units, with only minor amounts of dolomite. Backscattered SEM imaging proved to be very useful for finding dispersed quartz, iron oxides, and clay grains in the rather homogeneous field of calcite grains. We observed a notable spatial partitioning of the impurity mineral grains between the cores and the rinds of the oöids with the rinds apparently barren of non-calcite grains, and feel this distribution is a consequence of the Salem Limestone diagenesis.

The surface chemistry as measured by XPS is, of course, dominated by C, O, and Ca, but minor N, Na, Al, Si, P, S, Fe, Sn and Pb were also detected in all or some of the samples examined. The Al, Si, Fe, Sn, and Pb can be accounted for by impurity grains in the limestone. The Na and P were shown to be introduced by sample cleaning with in a mild soap solution; this cleaning step was later dropped. The adventitious nitrogen and carbon are found to be atmospheric contaminates confined to the surface-most atomic layers on the calcite grains. The carbon contaminantion, probably CO and $CO_2$, is found on all silicates, oxides, and carbonates exposed to air. The presence of adventitious nitrogen from air exposure is much less common.

The sulfur (in the form of sulfate) appears to be disseminated over the near-surface atomic layers of calcite grains throughout extended regions of the sample. Such contamination could have been introduced by ground water in the quarry. The presence of such disseminated sulfur in the freshly quarried Salem Limestone is a significant consideration in the ultimate interpretation of weathering data.

Because of the high degree of homogenity of the Salem Limestone, the dominant weathering process should involve a direct chemical attack on individual calcite grains without the influence of reaction products from the weathering of neighboring impurity grains in the limestone. A secondary weathering process conceivably might involve the redistribution of calcium sulfate by means of the leaching action of water passing through the stone. Such a mechanism is supported by the results of our analysis of the Washington National Cathedral stone yard sample. No sulfur or heavy metals (except small amounts of Fe) were detected in the XPS spectra, and there is no evidence that the surface of the grains in the Salem Limestone from the stone yard have been chemically altered due to acid rain.

In summary, the objectives of the NAPAP materials effects testing project are to identify mineralogical changes in building stones that have undergone exposure to weathering processes for various periods of time. The Salem Limestone control block appears to be an excellent choice of material for such a study since it provides a relatively homogeneous calcite matrix against which chemical alteration should be easily detected by XPS and SEM/EDX.

## REFERENCES

ASMUS J. F. (1978) Properties of laser-cleaned Carrara marble surfaces. Decay and preservation of stone (Eng. Geol. Case Hist. 11). The Geological Society of America, 3300 Penrose Place, Boulder, CO., p 81-88.

BANCROFT G. M., BROWN J. R. and FYFE W. S. (1979) Advances in, and applications of, X-ray photoelectron spectroscopy (ESCA) in mineralogy and geochemistry. Chemical Geology 25, 227-243.

BERNER R. A. and HOLDREN JR. G. R. (1979) Mechanism of feldspar weathering-II. Observations of feldspars from soils. Geochimica et Cosmochimica Acta 43, 1173-1186.

BERNER R. A. and SCHOTT J. (1982) Mechanism of pyroxene and amphibole weathering-II. Observations of soil grains. American Journal of Science 282, 1214-1231.

BISDOM E. B. A., HENSTRA S., KOOISTRA, M. J., van OOIJ W. J. and VISSER T. H. (1985) Combined high-resolution scanning Auger microscopy and energy dispersive x-ray analysis of soil samples. Spectrochimica Acta 40B, 879-884.

BOYLE R. H. (1983) Acid rain. Schocken Books, New York, 146 p.

BRAUN P., FARBER W., BETZ G. VIEHBOCK F. P. (1977) Effects in Auger electron spectroscopy due to the probing electrons and sputtering. Vacuum 27, no. 3, 103-108.

BUBENICK DAVID V., ed. (1984) Acid rain information book. Noyes Publications, Park Ridge, NJ, 397 p.

BUDIANSKY S. (1980) Acid rain and the missing link. Environmental Science and Technology 14, no. 10, 1172-1173.

BUDIANSKY S. (1981) Understanding acid rain. Environmental Science and Technology 15, no. 6, 623-624.

CARROLL D. (1970) Rock weathering. Plenum Press, New York, 203 p.

CARTER L. J. (1979) Uncontrolled $SO_2$ emissions bring acid rain. Science 204, no. 11, 1179-1182.

COGBILL C. V. (1976) The history and character of acid precipitation in eastern North America. Water, Air, Soil Pollution 6, nos. 2-4, 407-413.

COPPERTHWAITE R. G. (1980) Study of radiation induced chemical damage at solid surface using photoelectron spectroscopy: A review. Surf. Interface Anal. 2, 17-25.

DAVIES T. D. (1974) Dissolved sulphur dioxide and sulphate in urban and rural precipitation: Atomspheric Environment 13, no. 9, 1275-1285.

DAVISON J. I. and SEREDA P. J. (1978) Measurement of linear expansion in bricks due to freezing. Journal of Testing and Evaluation 6, no. 2, 144-147.

DEMEDIUK T. and COLE W.F. (1960) Contribution to the study of moisture expansion in ceramic materials. Journal of the American Ceramic Society 43, no. 7, 359-367.

DE PENA ROSA G. (1982) Sulfur in the atomosphere and its role in acid rain. Earth Miner. Sci. 51, 61-66.

DONAHUE J.D. (1967) Depositional Environments of the Salem Limestone (Mississippian, Meramec) of south-central Indiana, Indiana University Ph.D. dissertation, available from University Microfilms, Inc., Ann Arbor, MI.

DRUFUCA G. AND GIUGLIANO (1977) The duration of high $SO_2$ concentrations in an urban atmosphere. Atmospheric Environment 11, 729-735.

EFES Y. and LUCKAT S. (1976) Relations between corrosion of sandstones and uptake rates of air pollutants at the Cologne Cathedral. Second International Symposium on the Deterioration of Building Stones, Athens, Greece, 193-200.

FASSINA V., LAZZARINI G. and BISCONTIN G. (1976) Effects of atmospheric pollutants on the composition of black crusts deposited on Venetian marbles and stones. Second International Symposium on The Deterioration of Building Stones, Athens, Greece, 201-211.

FISHBURN C. C. (1940) Effects of wetting and drying on the permeability of masonry walls. National Bureau of Standards, Building Materials and Structures Report BMS55, 6p.

FORREST J., GARBER R. and NEWMAN L. (1979) Formation of sulfate, ammonium and nitrate in an oil-fired power plant plume. Atmospheric Environment, 13, 1287-1297.

FREDIANI P., MALESANI P. G. and VANNUCCI S. (1976) Weathering of Florentine stones: Sulfation and its determination. Second International Symposium on the Deterioration of Building Stones, Athens, Greece, 117-118.

FREEMAN I. L. (1966) Moisture expansion of structural ceramics. II The influence of composition. Transactions of the Tenth International Ceramic Congress, Stockholm, Sweden, 141-153.

FREEMAN I. L. (1967) Moisture expansion of structural ceramics. I Unrestrained expansion. Transactions of the British Ceramic Society, 66, no. 1, 13-35.

FURST M. (1974) The dynamics of weathering polish on sculptures of the Franconian baroque (rococo) and its significance. Geol. Bl. Nordost-Bayern 24, no. 1-2, 156-166.

GAURI K. L. (1980) Deterioration of architectural structures and monuments In Polluted Rain. (eds. T. Y. Toribara, M. W. Miller and P. E. Morrow), pp. 125-144. Plenum Press, New York.

GLASS N. R., ARNOLD D. E., GALLOWAY J. N., HENDREY G. R., LEE J. J., MC FEE W. M., NORTON S. A., POWERS C. F., RAMBO D. L. and SCHOFIELD C. L. (1982) Effects of acid precipitation. Environmental Science and Technology 16, no. 3, 162-169.

GLASS N. R., GLASS G. E. and RENNIE P. J. (1980) Effects of acid precipitation in North America. Environment International 4, 443-452.

GOUDIE A.S. (1977) Sodium sulphate weathering and the disintegration of Mohenjo-Daro, Pakistan. Earth Surface Processes 2, no. 1, 75-86.

HALES J. M. and DANA M. T. (1979) Regional-scale deposition of sulfur dioxide by precipitation scavenging. Atmospheric Environment 13, 1121-1132.

HEINEN H. J. and HOLM R. (1984) Recent developments with the laser microprobe mass analyzer (LAMMA). Scanning Electron Microscopy 1984, 1129-1138.

HERCULES D. M. 1976 electron spectroscopy: X-ray and electron excitation. Anal. Chem. 48: 295R-309R.

HERCULES S. H. and HERCULES D. M. (1974) Surface characterization by electron spectroscopy for chemical analysis (ESCA). In Characterization of solid surfaces. P. F. Kain and G. B. Larrabee (eds.), Plenum Press, N.Y.

HILEMAN B. (1981) Acid precipitation. Environmental Science and Technology 15, no. 10, 1119-1124.

HOCHELLA M. F., TURNER A. M. and HARRIS D. W. (1986a) High resolution scanning Auger microscopy of mineral surfaces. Scanning Electron Microscopy 1986 (in press).

HOCHELLA M. F., HARRIS D. W. and TURNER A. M. (1986b) High resolution scanning Auger microscopy as a high resolution microprobe for geologic materials-I. Techniques and demonstration. Am. Mineral. (in press).

HOFFMAN D., SCHIMMELWITZ P. and ROOSS H. (1976) Interactions of sulfur dioxide with lime plasters. Second International Symposium on the Deterioration of Building Stones, Athens, Greece, 37-42.

HOFFMANN M, R., MORGAN J. J., JACOB D. J., MUNGER J. W. and WALDMAN J. M. (1983) Characterization of reactants reaction mechanisms and reaction products leading to extrene acid rain and acid aerosol conditions in southern California. Environmental Engineering Science, W. M. Keck Laboratories, California Institute of Technology, Pasadena, California.

HOLDREN JR. G. R. and BERNER R. A. (1979) Mechanism of feldspar weathering-I. Experimental studies. Geochimica et Cosmochimica Acta 43, 1161-1171.

HUGHES R. E. and BARGH B. L. (1982) The weathering of brick: Causes, assessment and measurement. U.S. Geological Survey Open-File Report 83-272. Open-file services section, U.S.G.S, Branch of Distribution, Box 25425 Federal Center, Denver, CO 80225.

HUSAR R. B., LODGE J. P. MOORE, D. J., eds. (1977) Sulfur in the atmosphere. Proceedings of the International Symposium at Dubrovnik, Yugoslavia, Atmospheric Environment 12, 796 p.

JEANNETTE D. (1980) The sandstone of Landsberg Castle; an example for the evolution of the Vosges sands in a rural environment. Sci. Geol. Bull. 33, 111-118.

JOSHI A., DAVIS L. E. and PALMBERG P. W. (1975) Auger electron spectrometry. Methods of surface analysis, ed. Czanderna, A. W., Elsevier, New York.

KALISER B. N. (1976) Weathering of the Salt Lake City and County Building dimension stone. Utah Geol. Miner. Surv., 1-11.

KELLER, W. D. (1966) Geochemical weathering of rocks: source of raw materials for good living. Journal of Geol. Ed., 14, 17-22

LEWIN S. Z. and CHAROLA A. E. (1978) Scanning electron microscopy in the diagnosis of "diseased" stone. Scanning Electron Microscopy 1978, 695-702.

LIKENS G. E. and BORMANN F. H. (1974) Acid rain: a serious regional environmental problem. Science 184, 1176-1179.

LIKENS G. E., WRIGHT R. F., GALLOWAY J. N., and BUTLER, T. J. (1979) Acid rain. Scientific American 241, no. 4, p. 43-51.

LONGINELLI A. and BARTELLONI M. (1978) Atmospheric pollution in Venice, Italy, as indicated by isotopic analyses. Water, Air, and Soil Pollution 10, 335-341.

LOUGHNAN F. C. (1969) Chemical weathering of silicate minerals. Elsevier, New York, 154 p.

MACKINNON I. D. R. and MOGK D. W. (1985) Surface sulfur measurements of stratospheric particles. Geophysical Research Letters 12, 93-96.

MCKEEGAN K. D., WALKER R. M. and ZINNER E. (1985) Ion microscopic isotopic measurements of individual interplanatary dust particles. Geochimica et Cosmochimica Acta 49, 1971-1987.

MEIERDING T. E. (1981) Marble tombstone weathering rates. A Transect of The United States (unpublished report). Geography Department, University of Delaware, Newark, Delaware, 20 p.

MUCCI A., MORSE, J. W. and KAMINSKY M. S. (1985) Auger spectroscopy analysis of magnesian calcite overgrowths precipitated from sea water and solutions of sililar composition. American Journal of Science, 285, 289-305.

NAPAP, Annual report to the President and Congress (1983).
EOP Publications, Room 2200, 726 Jackson Place N.W., Washington, D.C. 20503

NRIAGU J. O., ed. (1978) Sulfur in the environment. Part II: Ecological impacts. New York: John Wiley and Sons, 482 p.

OLLIER C. D. (1984) Weathering. Elsevier, New York, 304 p.

PERRY D. L., TSAO L. and TAYLOR J. A. (1983) Surface studies of galena (PbS) using X-ray photoelectron spectroscopy and scanning Auger microscopy. Book of Abstracts, 185th American Chemical Society National Meeting.

PERRY D. L., TSAO L. and TAYLOR J. A. (1984) Surface studies of the interaction of copper ions with metal sulfide minerals. The Electrochemical Society Extended Abstracts Vol 84-1.

PETROVIC, R., BERNER R. A. and GOLDHABER M. B. (1976) Rate control in dissolution of alkali feldspars-I. Study of residual feldspar grains by X-ray photoelectron spectroscopy. Geochimica et Cosmochimica Acta 40, 537-548.

POUNDSTONE W. N. (1981) Let's get the facts on acid rain. Mining Congress Journal 66, no. 7, 45-47.

RABE H. (1984) Weathering damage to natural stone buildings. Der Aufschluss 35, 301-310.

RIGGS W. M. (1975) Surface analysis by X-ray photoelectron spectroscopy. In Methods of surface analysis, (ed. A. W. Czandera), Elsevier.

RIVIERE J. C. (1983) Auger techniques in analytic chemistry, The Analyst 108, 649-684.

ROSS M. and KNAB L. (1984) Selection, procurement, and description of Salem Limestone samples used to study effects of acid rain. National Bureau of Standards report NBSIR 84-2905, 17 p.

ROSSI-MANARESI R. (1976) Causes of decay and conservation treatments of the Tuff of Castel Dell'Ovo in Naples. Second International Symposium on the Deterioration of Building Stones, Athens, Greece, 233-247.

SCHOTT J. and BERNER R. A. (1983) X-ray photoelectron studies of the mechanism of iron silicate dissolution during weathering. Geochimica et Cosmochimica Acta 47, 2233-2240.

SCHOTT J., BERNER R. A. and SJÖBERG E. L. (1981) Mechanism of pyroxene and amphibole weathering-I. Experimental studies of iron-free minerals. Geochimica et Cosmochimica Acta 45, 2123-2135.

SEEGER P. (1968) Weathering of building and monumental stone. Naturhist. Ges. Hannover, Ber., Beih. 5, 35-37.

SEMONIN R. G. (1981) Acid rain: Is it a recent problem? Proceedings of the Illinois Mining Institute, Springfield, Illinois, 19-29.

SEQUEIRA R. (1981) Acid rain: some preliminary results from global data analysis. Geophys. Res. Lett. 8, no. 2, 147-150.

SHARP A. D., TRUDGILL S.T., COOKE R. U., PRICE C. A., CRABTREE R. W., PICKLES A. M. and SMITH D. I. (1982) Weathering of the balustrade on St. Paul's Cathedral, London. Earth Surfaces Processes and Landforms 7, no. 4, 387-389.

SHRINER D. S., RICHMOND C. R. and LINDBERG S. E. (1980) Atmospheric sulfur deposition--environmental impact and health effects. Proceedings of Second Life Sciences Symposium on Potential Environmental Impact and Health Effects of Atmospheric Sulfur Deposition in Gatlinburg, Tennessee, in 1979. Ann Arbor, Michigan: Ann Arbor Science Publishers, 568 p.

SIMON J. (1984) Acid rain. Prepared by the Congressional Research Service for the use of the Subcommittee on Health and the Environment of the Committee on Energy and Commerce, U.S. House of Representatives, Washington, D.C., 954 p.

SMITH N. M. (1962) Applied sedimentology of the Salem Limestone, Indiana University Ph.D. dissertation, available from University Microfilms, Inc., Ann Arbor, MI.

SMITH N. M. (1966) Sedimentology of the Salem Limestone in Indiana. Ohio Journal of Science 66, no. 2 p.168-179.

SOMMERS S. (1975) X-ray photoelectron spectra of Cls and Ols in carbonate minerals. Am. Mineral. 60, 483-484.

SPICER C. W. (1982) Nitrogen oxide reactions in the urban plume of Boston., Science 215, no. 4536, 1095-1096.

STEPHENSON D. A. and BINKOWSKI N. J. (1976) X-ray photoelectron spectroscopy of silica in theory and experiment. J. Non-cryst. Sol. 22, 399-421.

SUTTER J. F. and HARTUNG J. B. (1984) Laser microprobe $^{40}Ar/^{39}Ar$ dating of mineral grains in situ. Scanning Electron Microscopy 1984, 1525-1529.

VIKTOROV A. M. (1973) From stone to atmosphere. Priroda 2, 96-98.

WAGNER C. D., RIGGS W. M., DAVIS L. E. and MOULDER J. F. (1979) Handbook of X-ray photoelectron spectroscopy. G. E. Muilenberg (ed.), Physical Electronics Division, Perkin-Elmer Corp.

WINCHELL N. H. (1913) The weathering of aboriginal stone artifacts no. 1; a consideration of the paleoliths of Kansas. Minn. Hist. Soc. Collect. no. 16, part 1, 186 p.

WINKLER E. M. (1966) Important agents of weathering for building and monumental stone. Engineering Geology 1, no. 5, 381-400.

WINKLER E. M. (1973) Stone: Properties, Durability in Man's Environment, New York. Springer-Verlag, 230 p.

WINKLER E. M., ed. (1978) Decay and preservation of stone (Eng. Geol. Case Hist. 11). The Geological Society of America, 3300 Penrose Place, Boulder, CO.

TABLE I. Major Element Oxides

| | AU-3 | HU-3 | NU-3 |
|---|---|---|---|
| $SiO_2$ | .44 | .48 | .52 |
| $Al_2O_3$ | .19 | .18 | .17 |
| $Fe_2O_3$ | .10 | .13 | .12 |
| FeO | .02 | .01 | .01 |
| MgO | .44 | .47 | .47 |
| CaO | 56.2 | 55.4 | 55.5 |
| $Na_2O$ | .06 | .05 | .06 |
| $K_2O$ | .22 | .12 | .15 |
| $H_2O^+$ | .17 | .40 | .31 |
| $H_2O^-$ | .01 | .01 | .07 |
| $TiO_2$ | .01 | .01 | .01 |
| $P_2O_5$ | .01 | .03 | .03 |
| MnO | .01 | .02 | .02 |
| $CO_2$ | 43.2 | 42.7 | 43.5 |
| Total Percent | 101.06 | 99.99 | 100.93 |

TABLE II. Trace Element Constituents

| | AU-3 | HU-3 | NU-3 |
|---|---|---|---|
| Ag | .11 | .11 | .10 |
| Ba | 6.0 | 3.2 | 3.2 |
| Co | 1.7 | 1.3 | 1.5 |
| Cr | 3.7 | 6.0 | 1.6 |
| Cu | 1.1 | 1.0 | 1.0 |
| Mo | 2.9 | 2.9 | 3.0 |
| Ni | 3.8 | 3.2 | 2.5 |
| Sc | 3.5 | 3.1 | 3.8 |
| Sr | 500 | 540 | 510 |
| V | 6.2 | 4.5 | 6.9 |
| Y | 3.8 | 3.7 | 4.1 |
| Zr | 6.8 | 5.8 | 5.2 |

1. All concentrations are part-per-million.
2. Trace elements are determined using semi-quant optical emission spectrographic method. The precision of each valve is +.5 and -.33 of the amount reported.

# FIGURE CAPTIONS

Fig. 1. Differentiated and smoothed Auger electron spectra of study block sample HU-3. (a) Electron beam rastered over 2 x 2 mm area of sample. (b) Electron beam stationary (0.02 um diameter beam). Note absence of carbon line.

Fig. 2. Scanning electron micrograph of NU-3 at (a) 50X and (b) at 200X showing Salem Limestone oöids.

Fig. 3. Scanning electron micrograph of NC-1 (Salem Limestone sample from Washington National Cathedral) at 50X .

Fig. 4. Scanning electron micrographs of NU-3 at 2500X showing (a) SEM image and (b) backscattered electron image of same area as (a). Note Fe-rich grain and silica fossil fragment. EDX showed only iron in the inclusion and silicon in the fossil fragment.

Fig. 5. Survey X-ray photoelectron spectrum of HU-3 (60-190 eV and 275-295 eV regions are expanded in Figs. 6 and 7, respectively).

Fig. 6. Narrow band X-ray photoelectron spectra of HU-3. See text for explanation.

Fig. 7. Narrow band X-ray photoelectron spectra of HU-3 showing carbon 1s lines. The line at 289 eV is due to the carbon in the calcite carbonate group; the line at 284 eV is due to contamination from air exposure.

Fig. 8. Narrow band X-ray photoelectron spectra of sample HU-3 (a) before sputtering, and (b) after 30 seconds of sputtering with $Ar^+$ at 4 kV. Note decrease in sulfur line intensity relative to silicon line intensity after sputtering.

## ACKNOWLEDGEMENTS

We wish to thank Malcolm Ross and Elaine McGee (U.S. Geol. Survey) for furnishing samples of the Salem Limestone and for their advice throughout this work. We also wish to acknowledge the following people for their advice and assistance with the instrumental analytical work:

Robert L. Oscarson, Paul Hearn, Robert Johnson and Hezekiah Smith (U.S. Geol. Survey)

William F. Stickle, Arthur M. Turner, David W. Harris, and Lap S. Chan (Physical Electronics Laboratories, Mt. View, CA)

Filippo Radicati di Brozolo and Charles J. Hitzman (Evans and Associates, San Mateo, CA)

This research has been funded as part of the National Acid Precipitation Assessment Program by the National Park Service, U.S. Department of Interior.

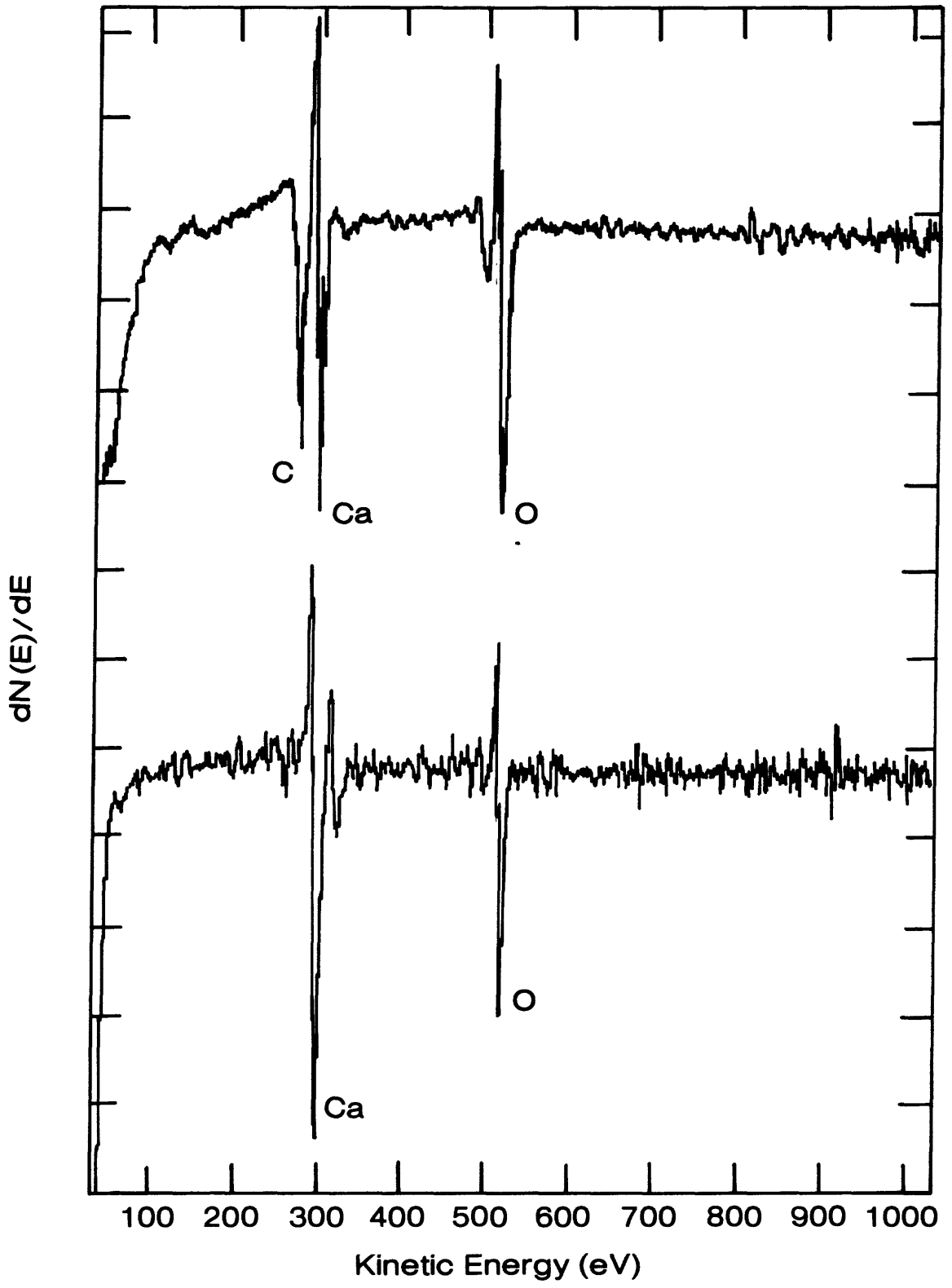


Fig. 1. Differentiated and smoothed Auger electron spectra of study block sample HU-3. (a) Electron beam rastered over 2 x 2 mm area of sample. (b) Electron beam stationary (0.02 um diameter beam). Note absence of carbon line.

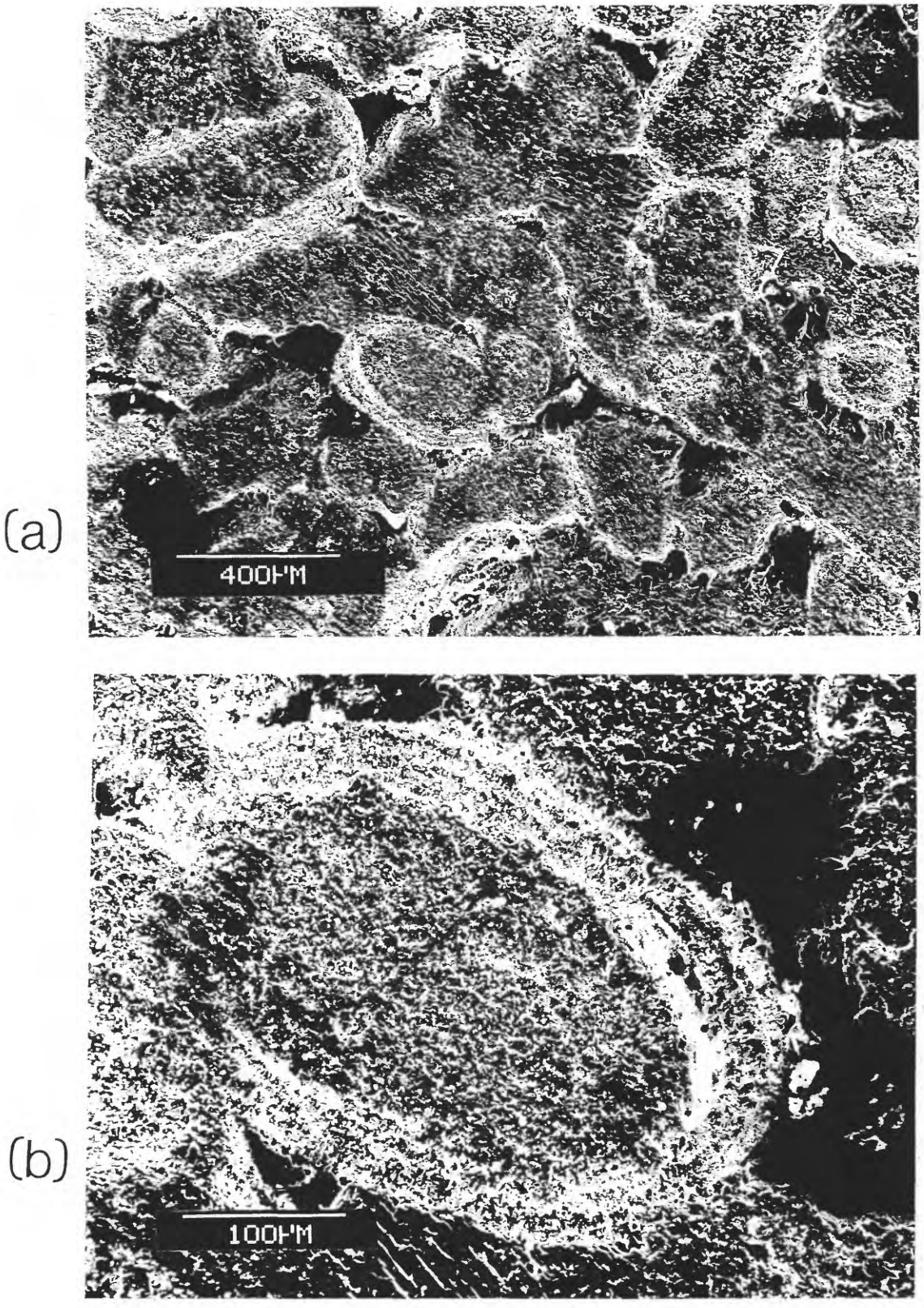


Fig. 2. Scanning electron micrograph of NU-3 at (a) 50X and (b) at 200X showing Salem Limestone oöids.

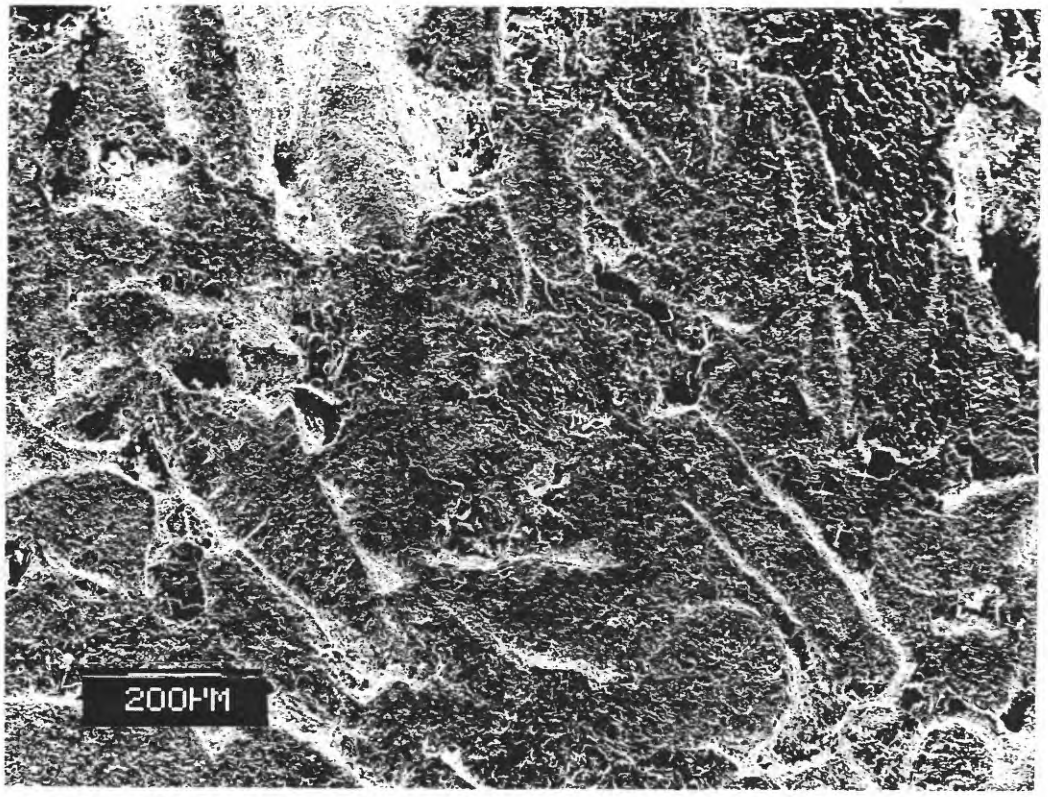


Fig. 3. Scanning electron micrograph of NC-1 (Salem Limestone sample from Washington National Cathedral) at 50X .

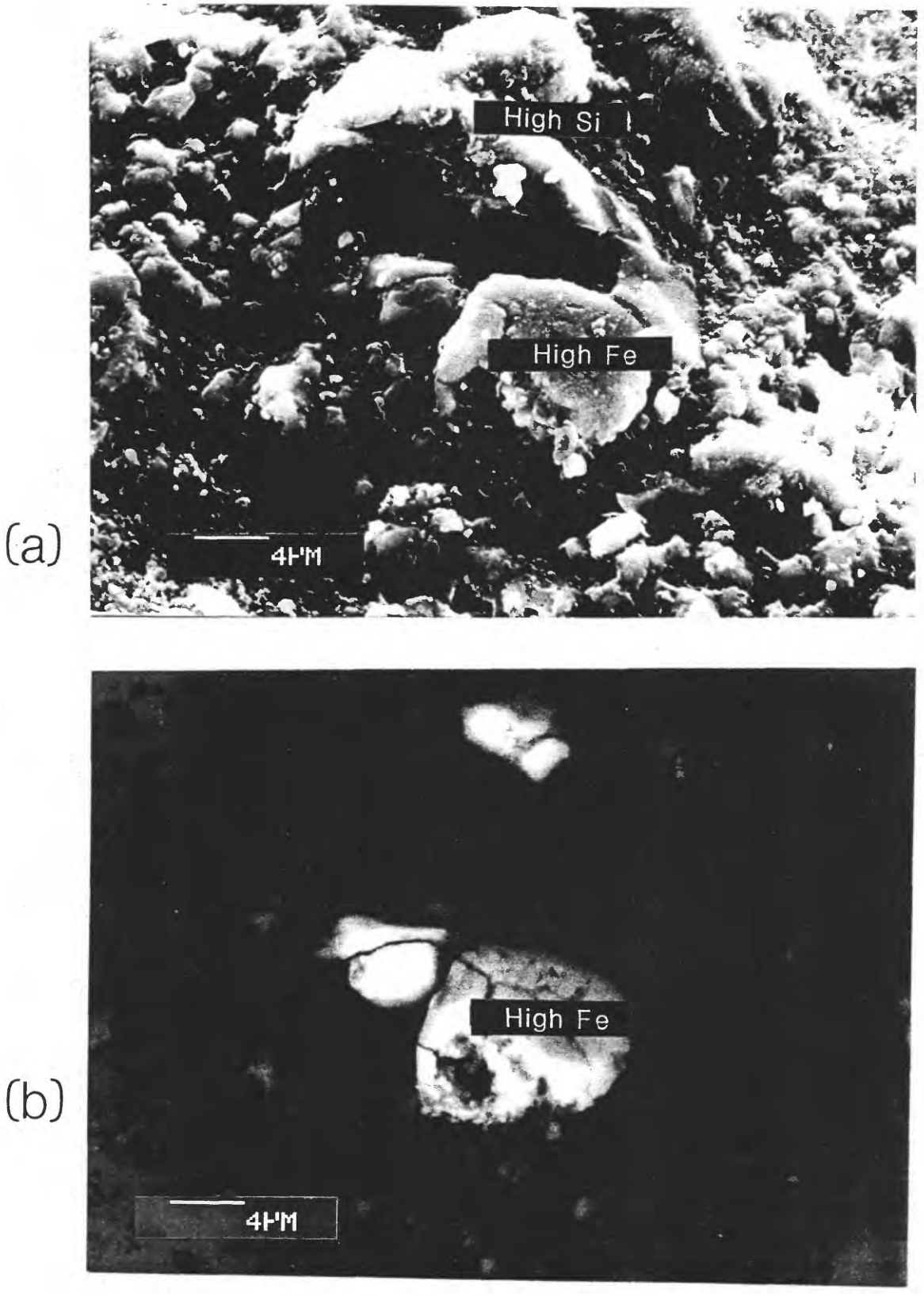


Fig. 4. Scanning electron micrographs of NU-3 at 2500X showing (a) SEM image and (b) backscattered electron image of same area as (a). Note Fe-rich grain and silica fossil fragment. EDX showed only iron in the inclusion and silicon in the fossil fragment.

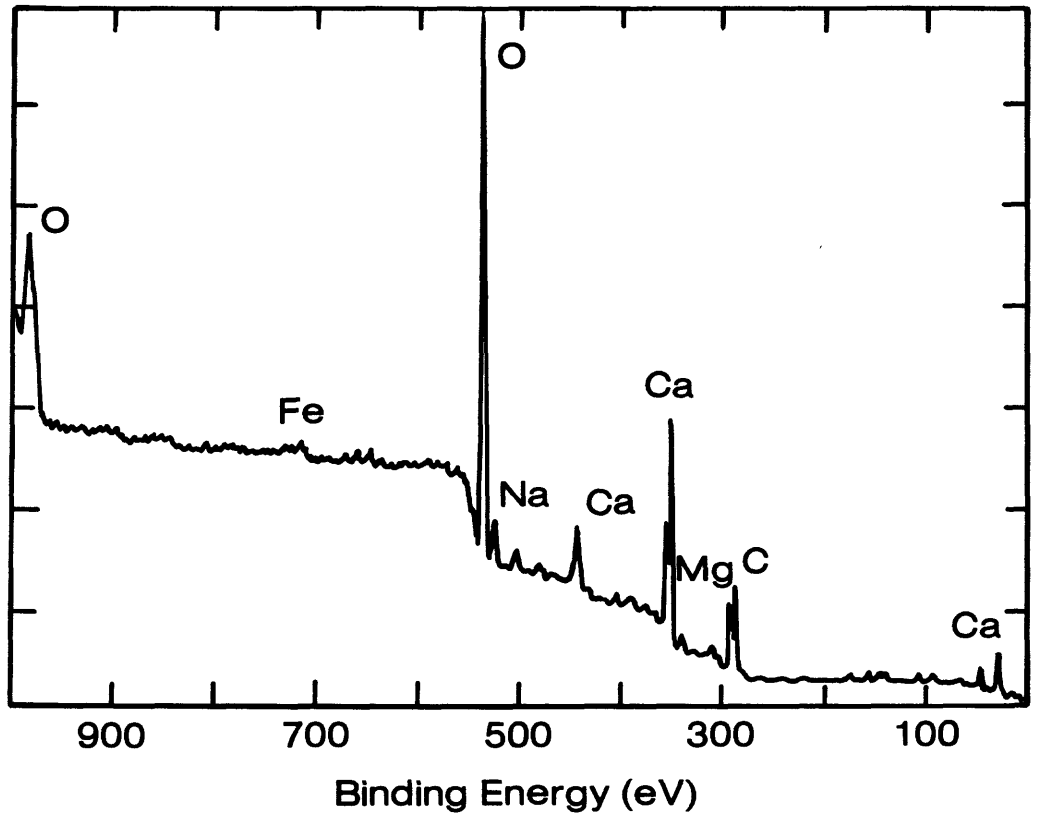


Fig. 5. Survey X-ray photoelectron spectrum of HU-3 (60-190 eV and 275-295 eV regions are expanded in Figs. 6 and 7, respectively).

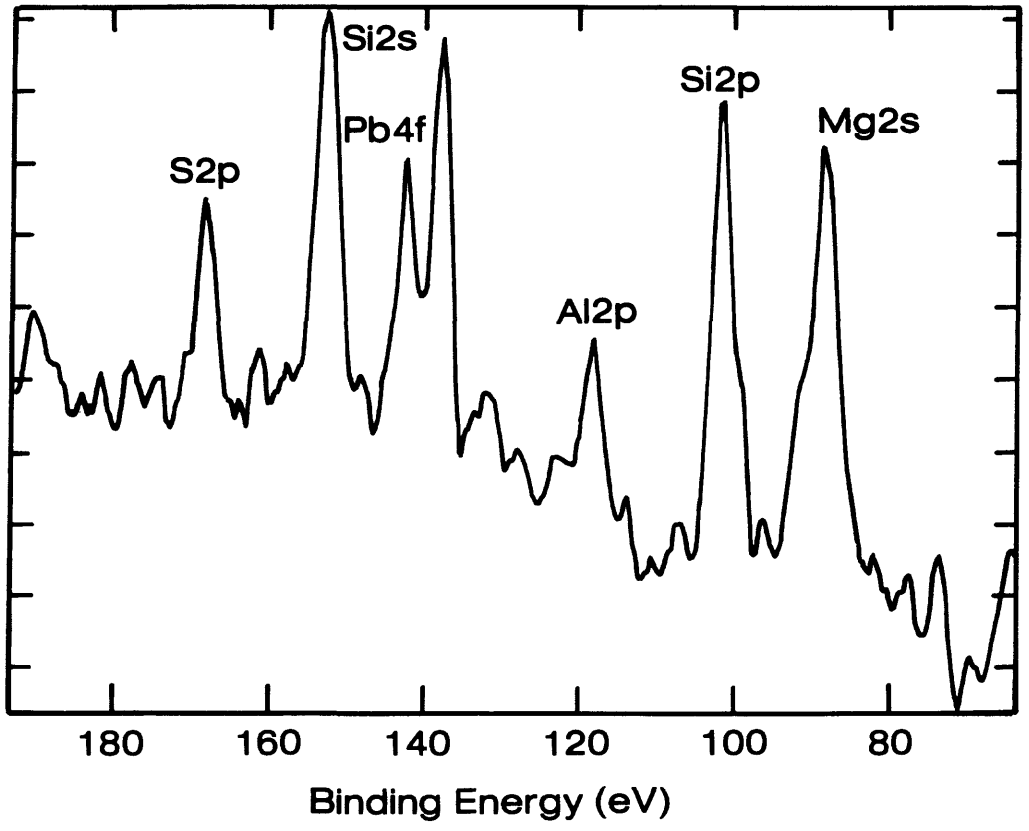


Fig. 6. Narrow band X-ray photoelectron spectra of HU-3. See text for explanation.

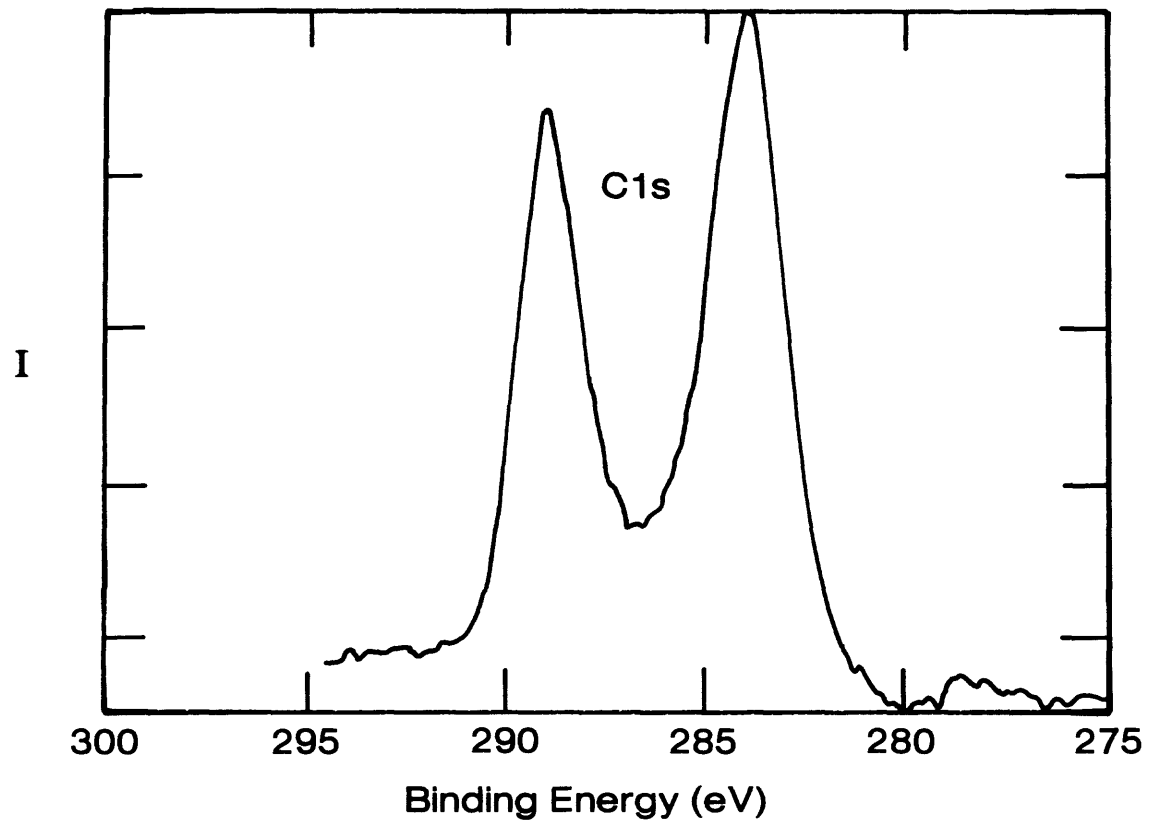


Fig. 7. Narrow band X-ray photoelectron spectra of HU-3 showing carbon 1s lines. The line at 289 eV is due to the carbon in the calcite carbonate group; the line at 284 eV is due to contamination from air exposure.

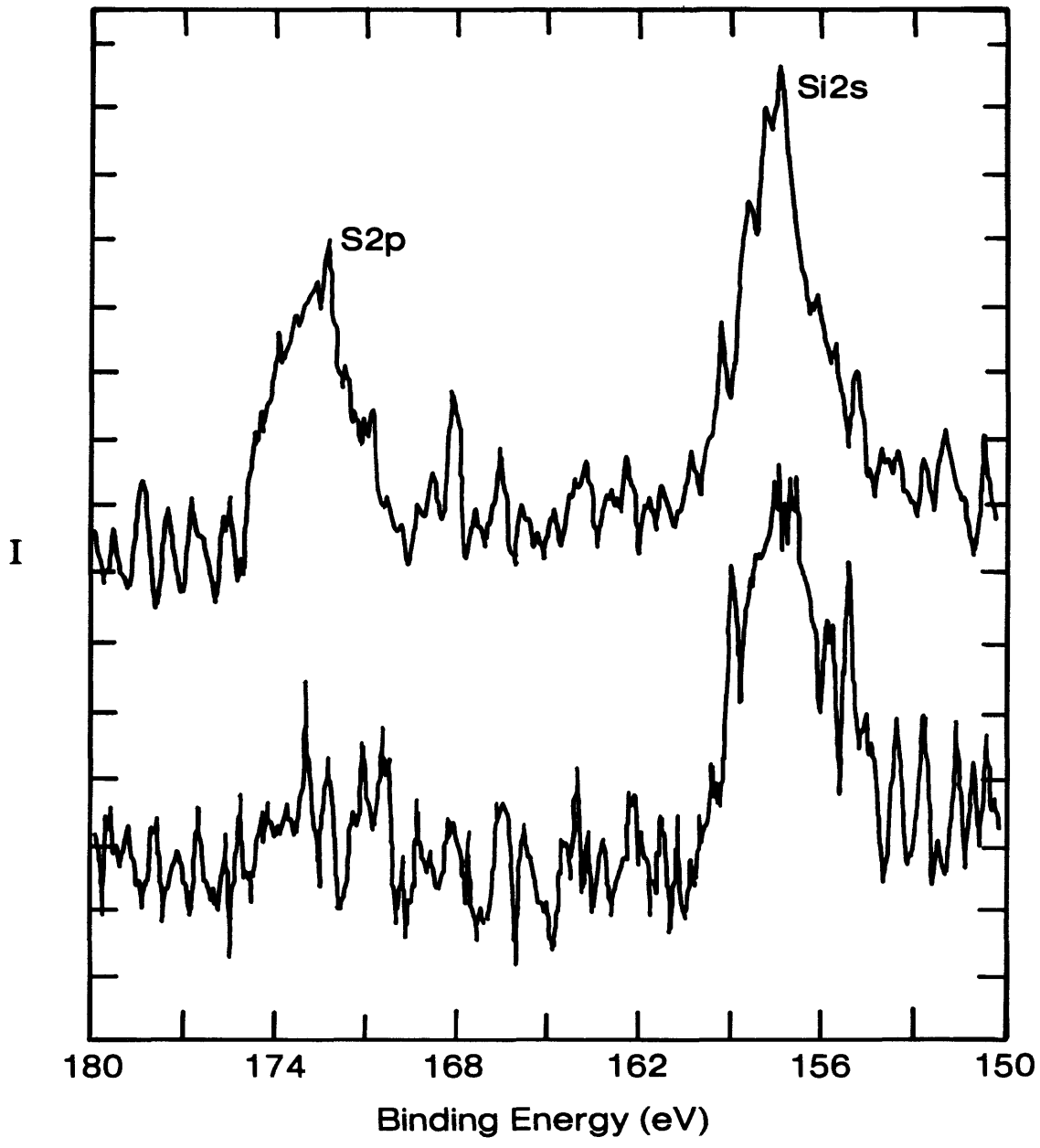


Fig. 8. Narrow band X-ray photoelectron spectra of sample HU-3 (a) before sputtering, and (b) after 30 seconds of sputtering with $Ar^+$ at 4 kV. Note decrease in sulfur line intensity relative to silicon line intensity after sputtering.